Mass function and bias of dark matter halos

0905.2277

0906.1042

Invisible Universe, July 2nd, 2009

P. Valageas, IPhT Saclay, France

Probability distribution of rare events

Gaussian linear density contrast: $\delta_L(\mathbf{q})$

linear two-point correlation: $C_L(\mathbf{q}_1, \mathbf{q}_2) = \langle \delta_L(\mathbf{q}_1)\delta_L(\mathbf{q}_2)\rangle$

probability distribution of the nonlinear density contrast δ_r within spherical cells of radius r $\quad \mathcal{P}(\delta_r)$

rare events: $\quad \mathcal{P}(\delta) \sim \max_{\{\delta_L[\mathbf{q}]|\delta_r[\delta_L]=\delta\}} e^{-\frac{1}{2}\delta_L.C_L^{-1}.\delta_L}$

nonlinear constraint

Gaussian weight

Radial profile of the saddle-point

Lagrangian to Eulerian mapping

$$q'^3 = (1+\delta'_r) r'^3 \quad \text{with} \quad \delta_{r'} = \mathcal{F}(\delta_{Lq'})$$

spherical dynamics

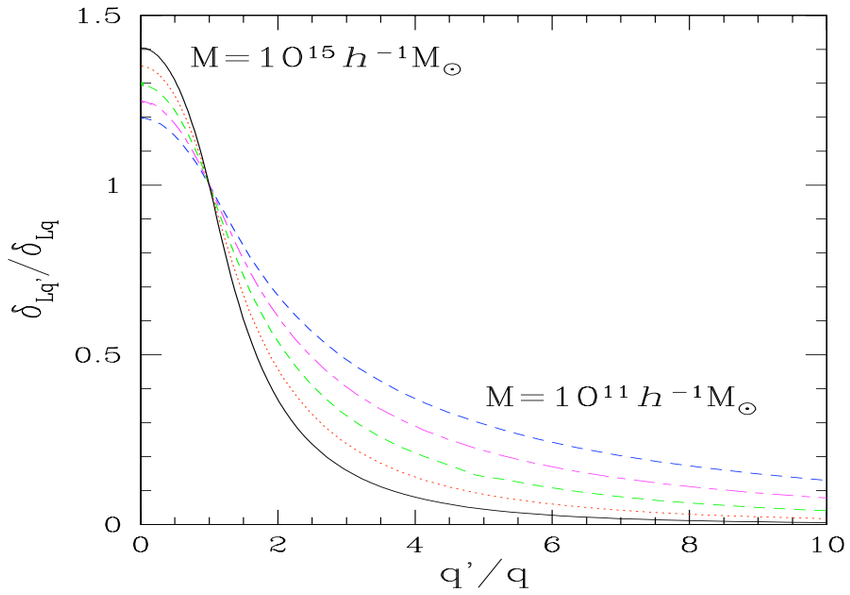

$$\delta_{Lq'} = \delta_{Lq} \frac{\sigma^2_{q,q'}}{\sigma^2_q}$$

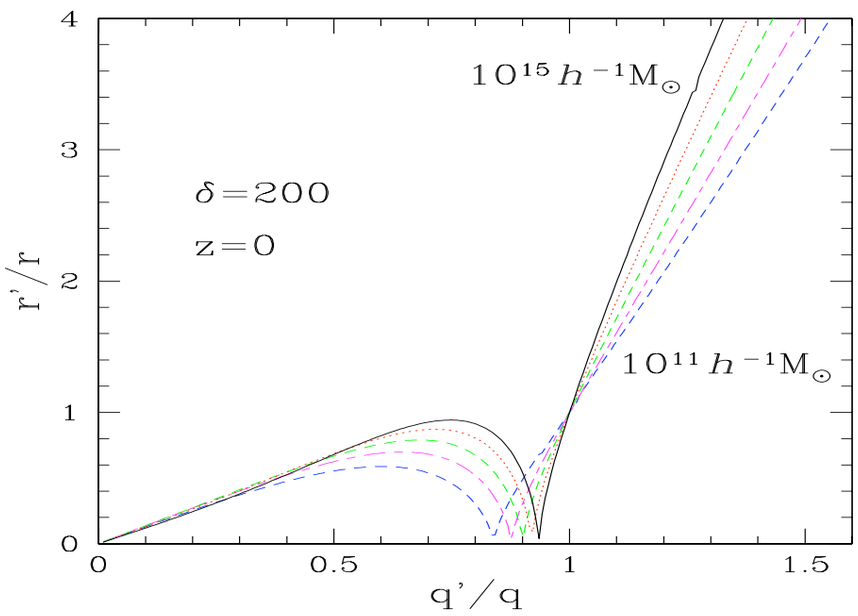

upper bound due

to shell-crossing

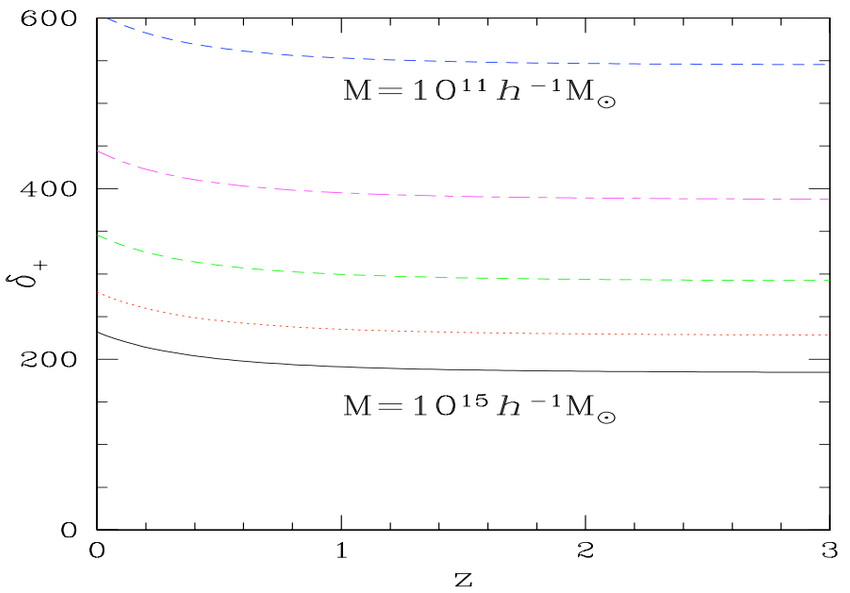

Phase-space diagram of dark matter halos

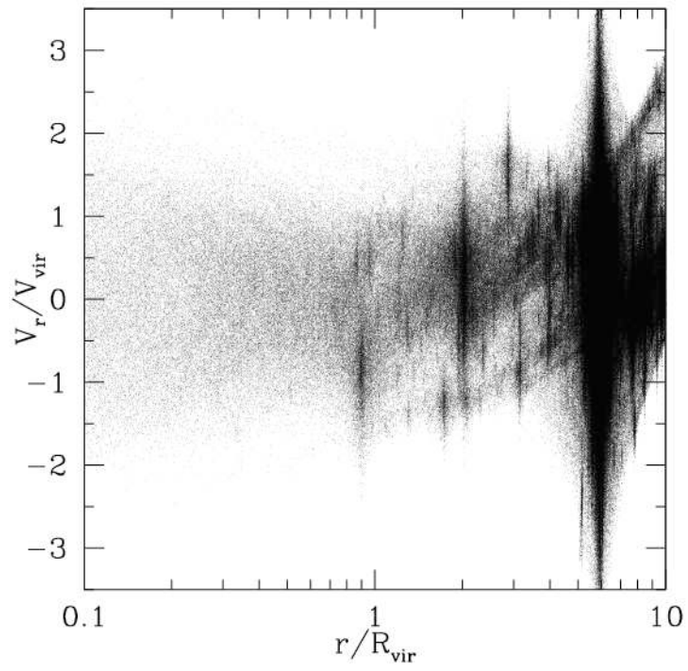

Cuesta et al. (2008)

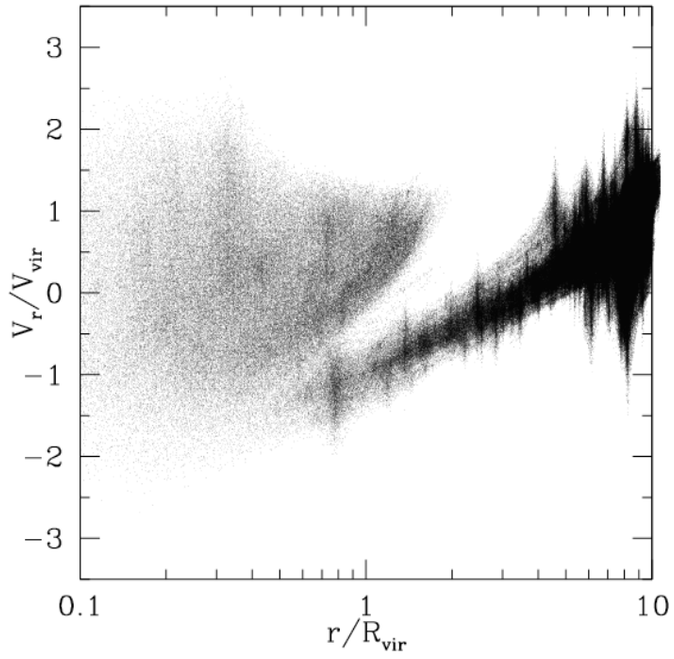

$2.9 \times 10^{11} h^{-1} M_\odot$

$1.3 \times 10^{15} h^{-1} M_\odot$

linear density contrast δ_L associated with spherical regions of nonlinear density contrast $\Delta = 200$

Robertson et al. (2009)

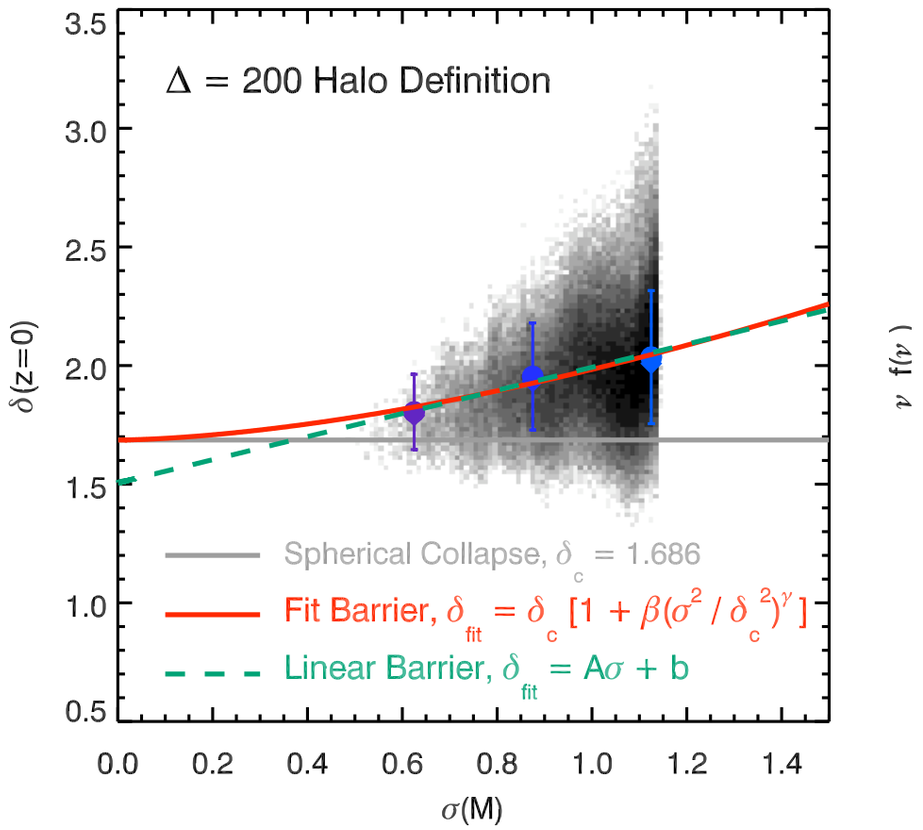

Mass function of collapsed halos

The large-mass exponential cutoff remains the same

$$M \to \infty : \quad \ln[n(M)] \sim -\frac{\delta_L^2}{2\sigma^2}, \qquad \text{with} \quad \delta_L = \mathcal{F}^{-1}(\delta)$$

For instance, one can use $n(M)dM = \frac{\bar{\rho}_m}{M} f(\nu) \frac{d\nu}{\nu}$ with

$$\nu = \frac{\delta_L}{\sigma}, \quad \delta_L = \mathcal{F}^{-1}(\delta) \simeq 1.59 \ \text{ for } \ \delta = 200, \quad \Omega_m = 0.27$$

and $\nu \to \infty : \quad f(\nu) \sim e^{-\nu^2/2}$

Normalization: $\int_0^\infty f(\nu) \frac{d\nu}{\nu} = 1$

Sheth & Tormen (1999)
Jenkins et al. (2001)
Reed et al. (2003)
Warren et al. (2006)
Tinker et al. (2008)

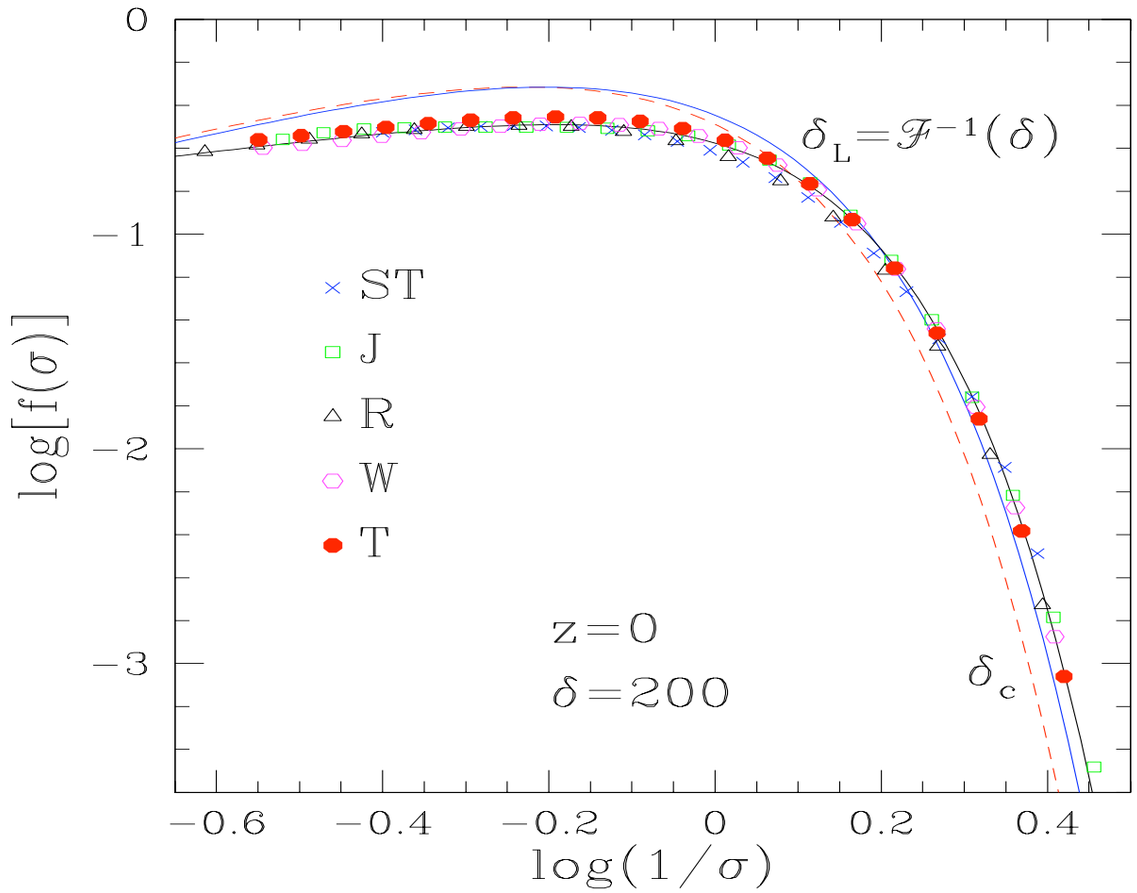

$$f_{\rm PS}(\nu) = \sqrt{\frac{2}{\pi}}\,\nu\,e^{-\nu^2/2}$$

Press-Schechter (1974) with

$\delta_L \simeq 1.59$

$$f(\nu) = 0.5\left[(0.6\,\nu)^{2.5} + (0.62\,\nu)^{0.5}\right]\,e^{-\nu^2/2}$$

fit normalized to unity

Halo density profile

overdensity within radius r

Prada et al. (2006)
Betancort-Rijo et al. (2006)

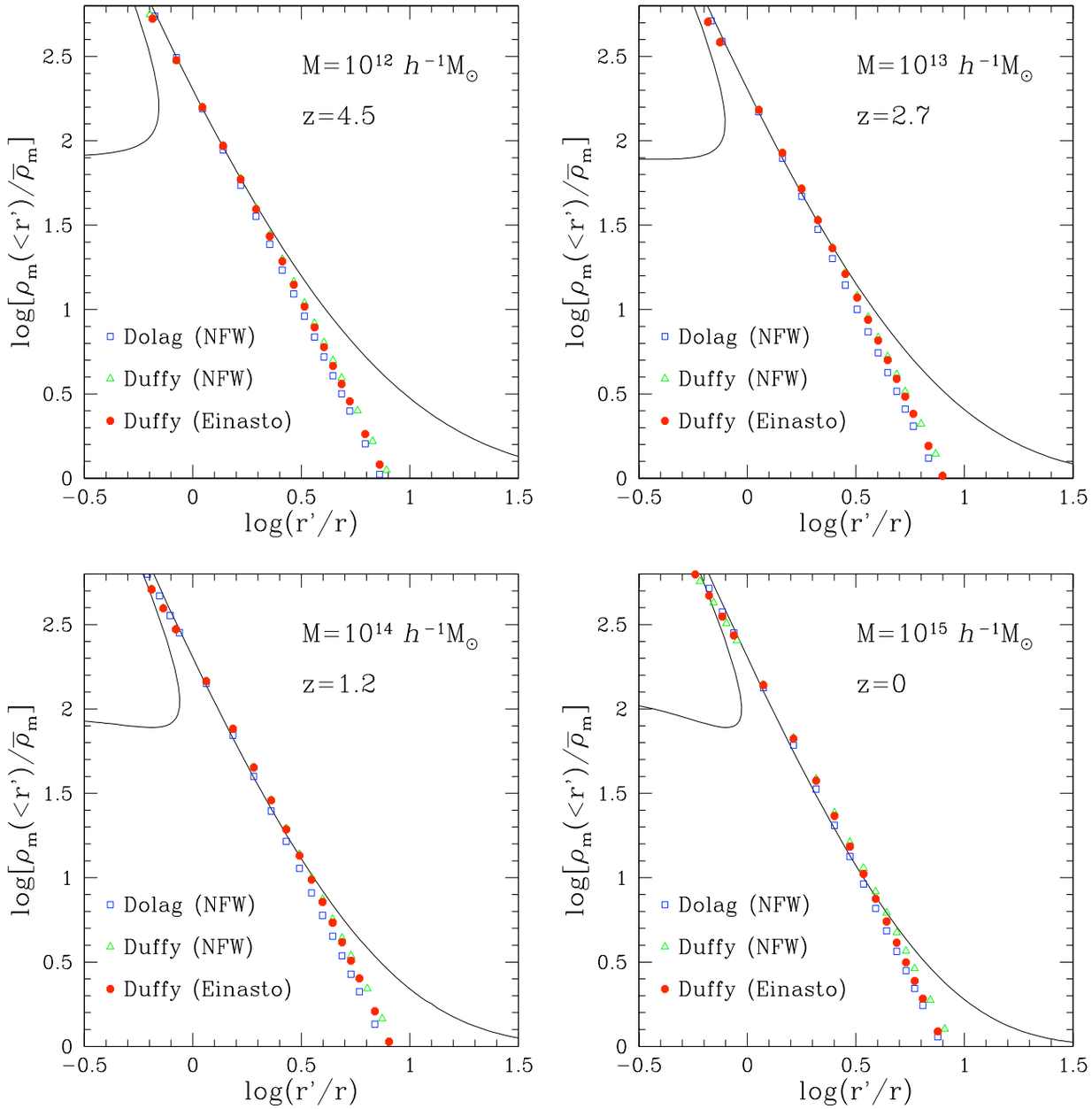

Dolag et al. (2004)
Duffy et al. (2008)

Halo bias

For two Eulerian cells we again have in the limit of rare events

$$\mathcal{P}(\delta_{r_1}, \delta_{r_2}) \sim e^{-\frac{1}{2}\delta_L . C_L^{-1} . \delta_L}$$

As in Kaiser (1984), this leads to the approximation:

$$1 + \xi_{M_1,M_2}(x) \sim (1 + \delta_M(x)) \frac{\mathcal{P}_L(\delta_{L1}, \delta_{L2})}{\mathcal{P}_L(\delta_{L1})\mathcal{P}_L(\delta_{L2})}$$

Lagrangian to Eulerian mapping

correlation of high peaks in the linear field

Taking into account the displacements of halos:

$$q \simeq r\left(1 + \frac{\delta_r}{3}\right) \quad \Rightarrow \quad x \simeq q\left(1 - \frac{\delta_L}{3}\frac{\sigma^2_{q_1,s}}{\sigma^2_{q_1}} - \frac{\delta_L}{3}\frac{\sigma^2_{q_2,s}}{\sigma^2_{q_2}}\right)$$

test particle

pair separation

Real-space bias:

$$b^2_{M_1,M_2}(r) = \frac{\xi_{M_1,M_2}(r)}{\xi(r)}$$

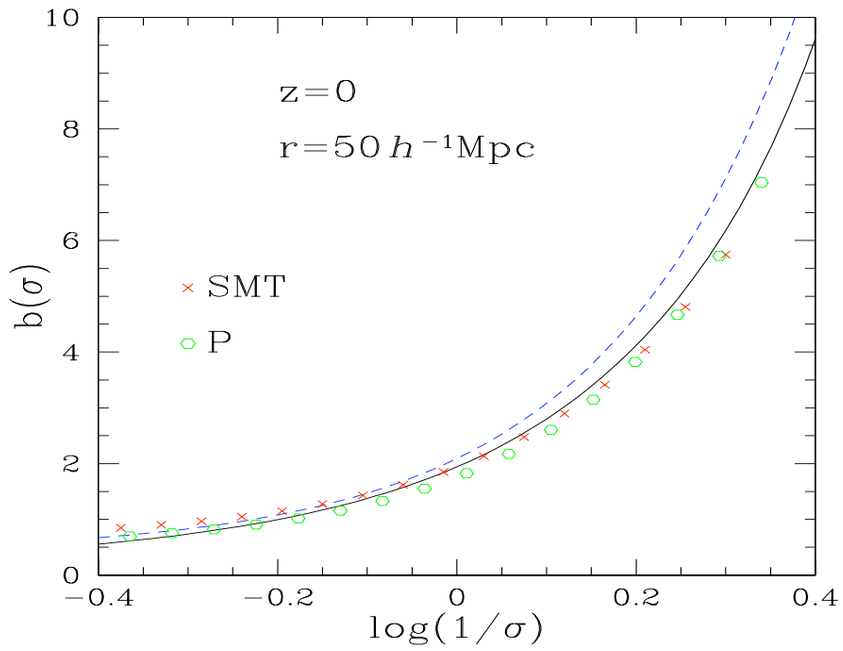

Halo bias $b(M)$ as a function of $\sigma(M)$

Mo & White (1996) (dashed)
Sheth, Mo & Tormen (2001)
Pillepich et al. (2009)

Halo bias $b(r)$ as a function of distance r at $z = 0$ and $z = 10$

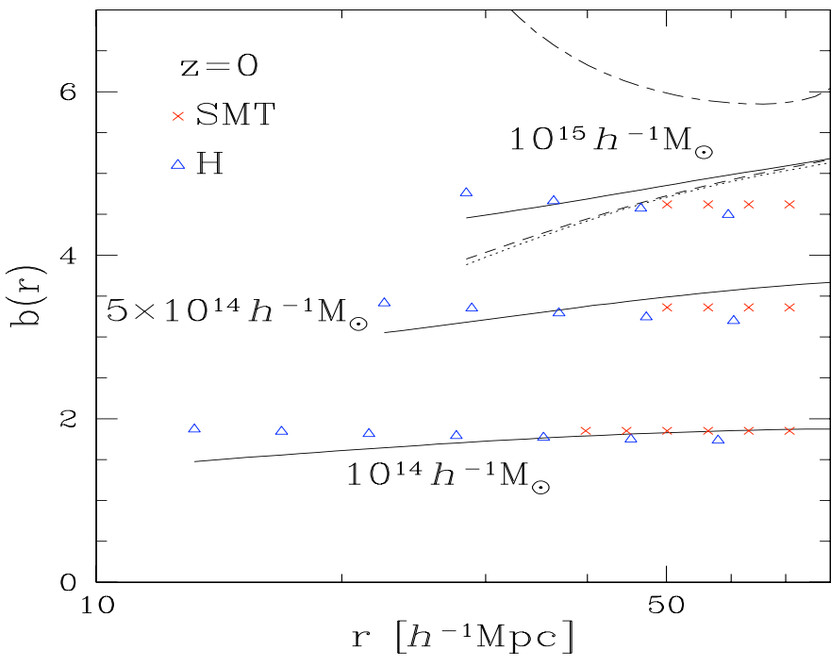

Hamana et al. (2001)

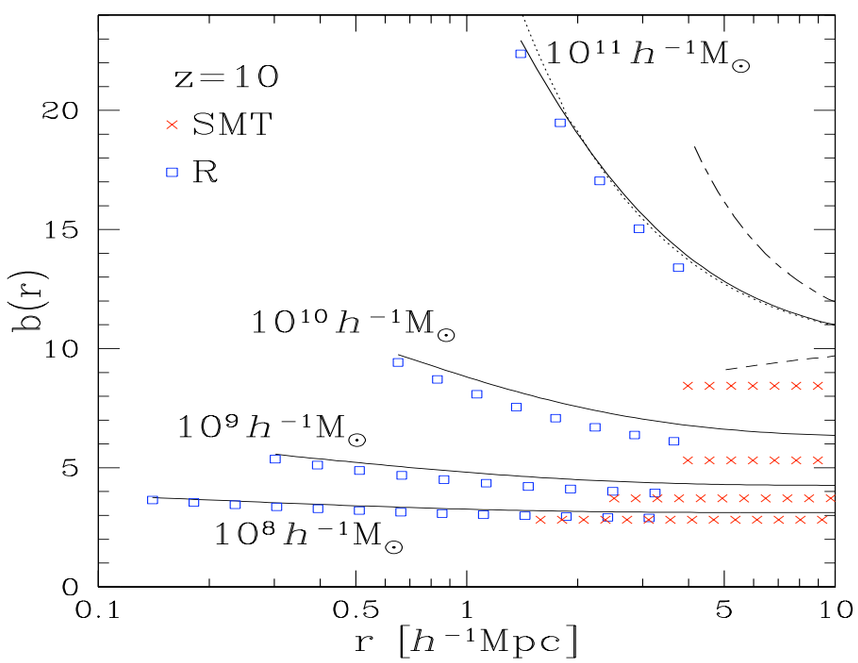

Reed et al. (2009)

Non-Gaussian initial conditions

local type: $\Phi(\mathbf{x}) = \phi(\mathbf{x}) + f_{\rm NL}(\phi(\mathbf{x})^2 - \langle\phi^2\rangle)$

Gaussian

Poisson eq. $\Rightarrow$ $\tilde{\delta}_L(\mathbf{k},z) = \alpha(k,z)\tilde{\Phi}(\mathbf{k})$ with $\alpha(k,z) = \dfrac{2c^2k^2T(k)D(z)}{3\Omega_m H_0^2}$

Defining $\tilde{\chi}(\mathbf{k},z) = \alpha(k,z)\tilde{\phi}(\mathbf{k})$ gives

$$\tilde{\delta}_L(\mathbf{k}) = \tilde{\chi}(\mathbf{k}) + \int d\mathbf{k}_1 d\mathbf{k}_2\, \delta_D(\mathbf{k}_1+\mathbf{k}_2-\mathbf{k})\, \tilde{f}^{\delta}_{\rm NL}(\mathbf{k}_1,\mathbf{k}_2)\tilde{\chi}(\mathbf{k}_1)\tilde{\chi}(\mathbf{k}_2)$$

local type: $\tilde{f}^{\delta}_{\rm NL}(\mathbf{k}_1,\mathbf{k}_2) = \dfrac{\alpha(\mathbf{k}_1+\mathbf{k}_2)}{\alpha(k_1)\alpha(k_2)}$

Rare events

$$\mathcal{P}_L(\delta_L) \sim \max_{\{\chi[\mathbf{q}]|\delta_{Lq}=\delta_L\}} e^{-\frac{1}{2}\chi.C_L^{-1}.\chi}$$

$$\Rightarrow \quad \mathcal{P}_L(\delta_L) \sim e^{-\frac{\delta_L^2}{2\sigma_q^2}\left(1-\frac{\delta_L}{3}S_3\right)}$$

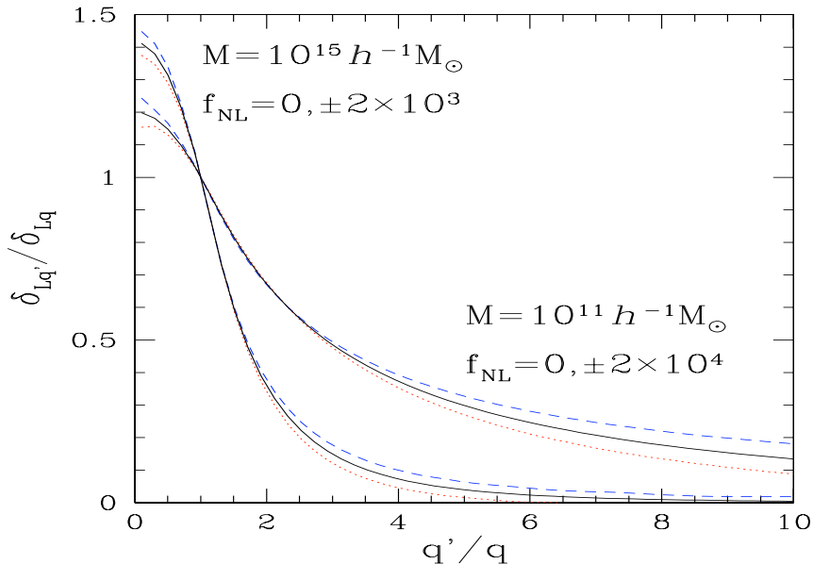

saddle point with a profile close to the Gaussian one

same value for the shell-crossing bound δ_+

$$f_{\rm NL}=0: \qquad n(M,0)dM = \frac{\bar{\rho}_m}{M} f(\nu)\frac{d\nu}{\nu} \quad \text{with} \quad \nu = \frac{\delta_L}{\sigma(M)}$$

$$f_{\rm NL}\neq 0: \quad \begin{cases} n(M,f_{\rm NL}) = n(M,0)\, e^{S_3\delta_L^3/(6\sigma_q^2)} \\ n(M,f_{\rm NL})dM = \dfrac{\bar{\rho}_m}{M} f(\mu)\dfrac{d\mu}{\mu} \end{cases} \quad \textbf{with} \quad \mu = \frac{\delta_L}{\sigma(M)}\sqrt{1-\frac{\delta_L}{3}S_3(M)}$$

Afshordi & Tolley (2009)
Matarrese et al. (2000)

$\Rightarrow$ mass function normalized to unity

Ratio of non-Gaussian to Gaussian mass functions

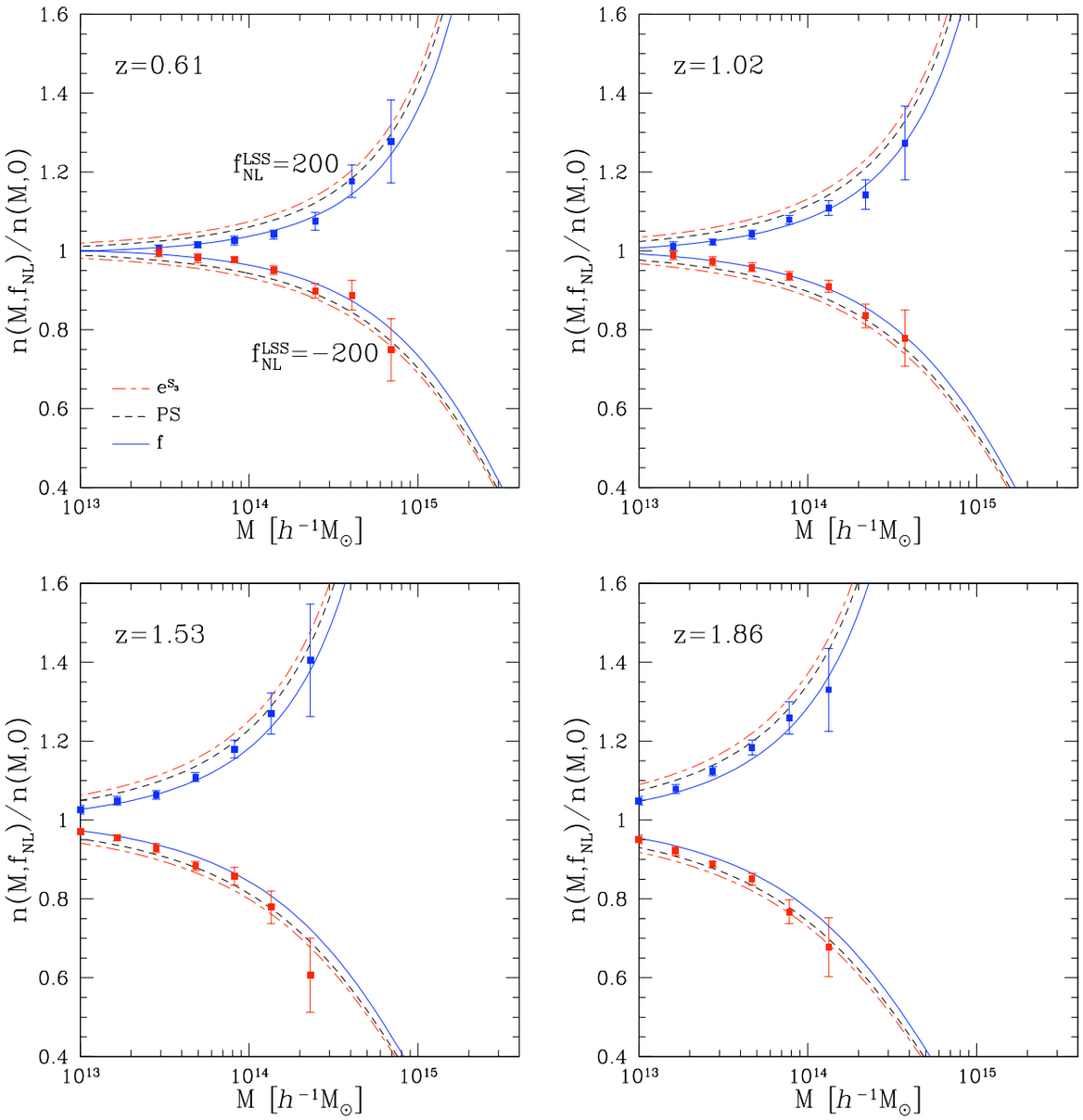

Grossi et al. (2009)

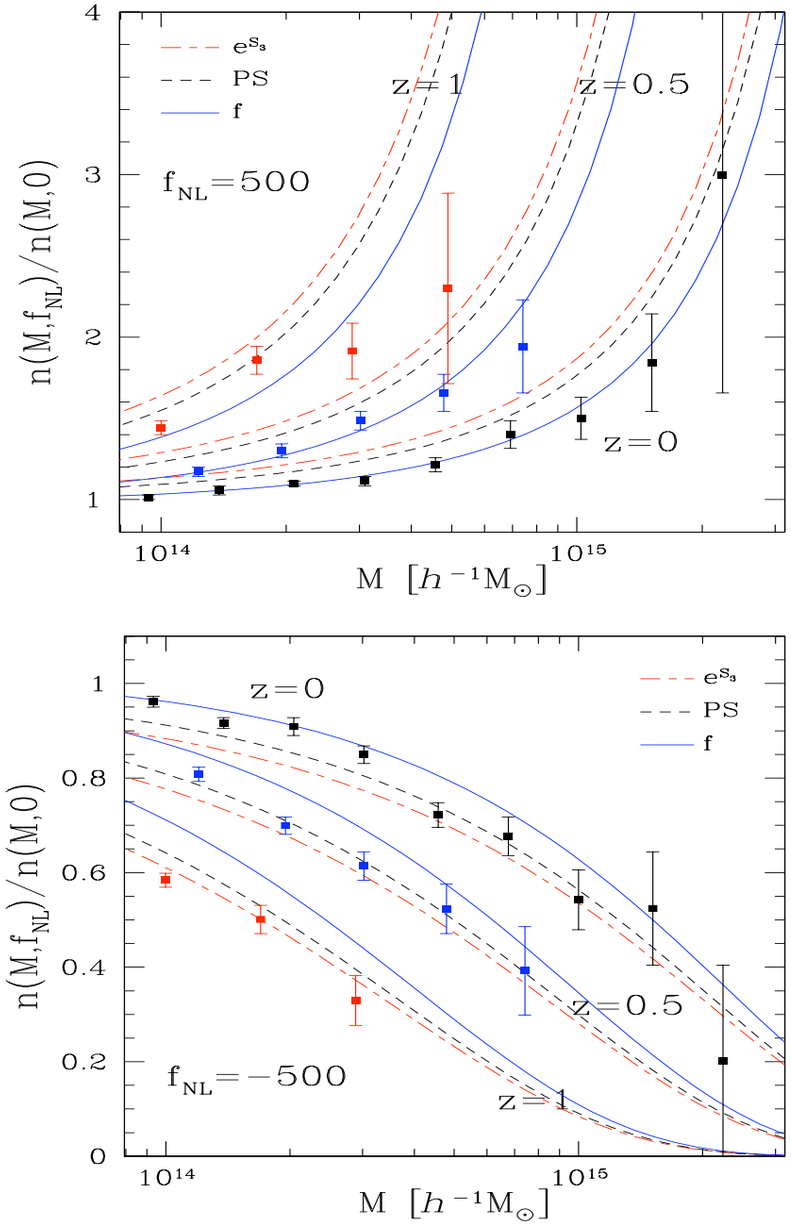

Dalal et al. (2008)

Halo bias

$$\mathcal{P}_L(\delta_{L1},\delta_{L2}) \sim \mathcal{P}_L(\delta_{L1})\mathcal{P}_L(\delta_{L2})\, e^{-\Delta\Gamma}$$

whence

$$1+\xi_{M_1,M_2}(x) \sim (1+\delta_M(x))\, e^{-\Delta\Gamma}$$

$$x\to\infty: \quad \xi_M(x) \sim \frac{\delta_L}{\sigma_q^2}\sigma_{q,0}^2(s) + \frac{\delta_L^2}{\sigma_q^4}\left[f_{0;qq}(s)+2f_{q;0q}(s)-3\frac{f_{q;qq}}{\sigma_q^2}\sigma_{q,0}^2(s)\right]$$
$$+\frac{\delta_L^2}{\sigma_q^4}\sigma_{q,q}^2(s)+2\frac{\delta_L^3}{\sigma_q^6}\left[f_{2;11}(s)+2f_{1;12}(s)-3\frac{f_{1;11}}{\sigma_q^2}\sigma_{q,q}^2(s)\right]$$

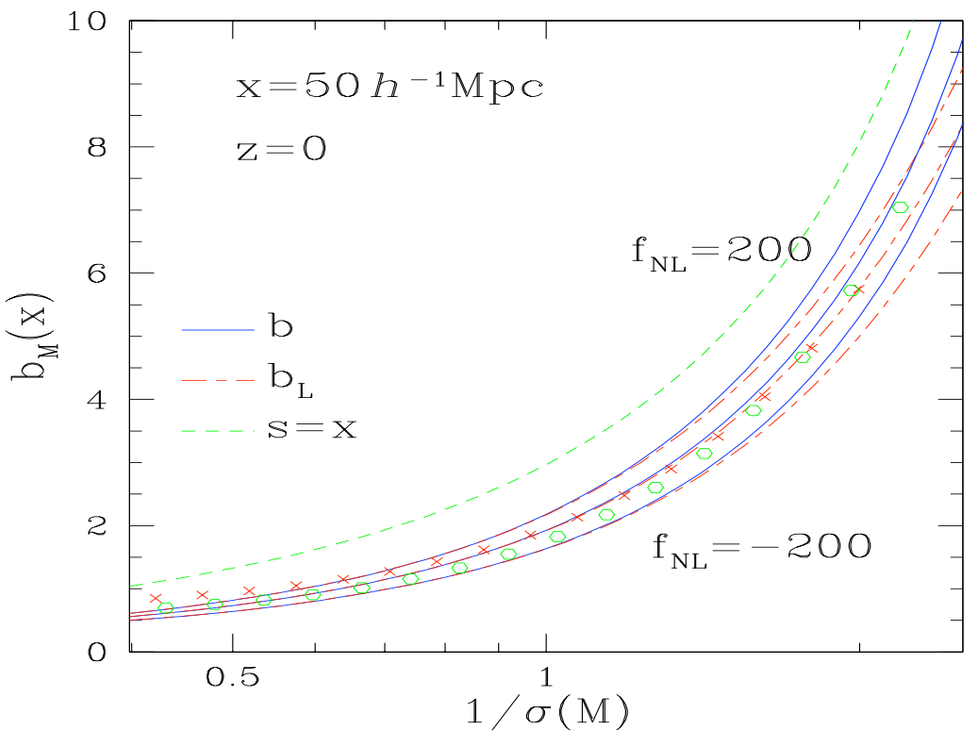

Real-space bias

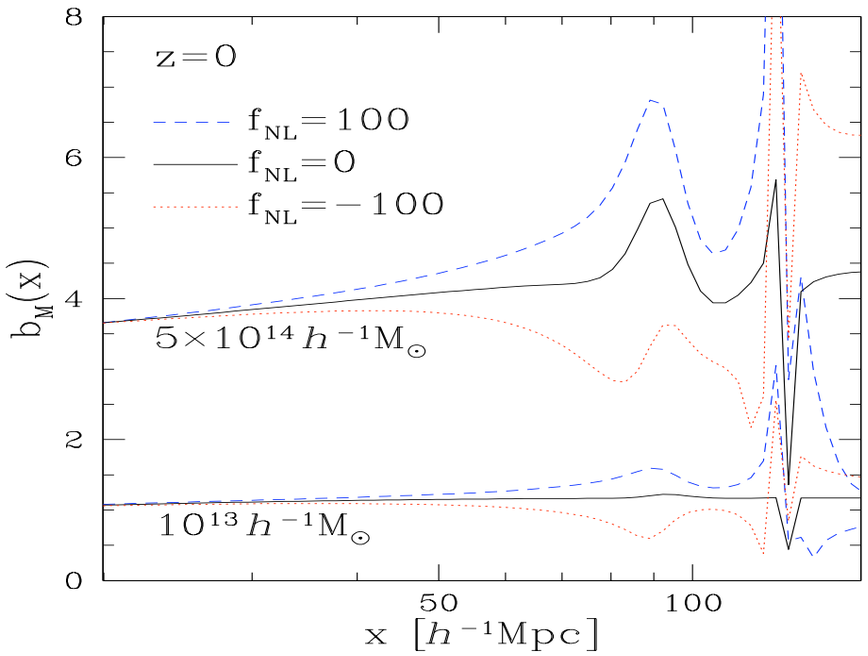

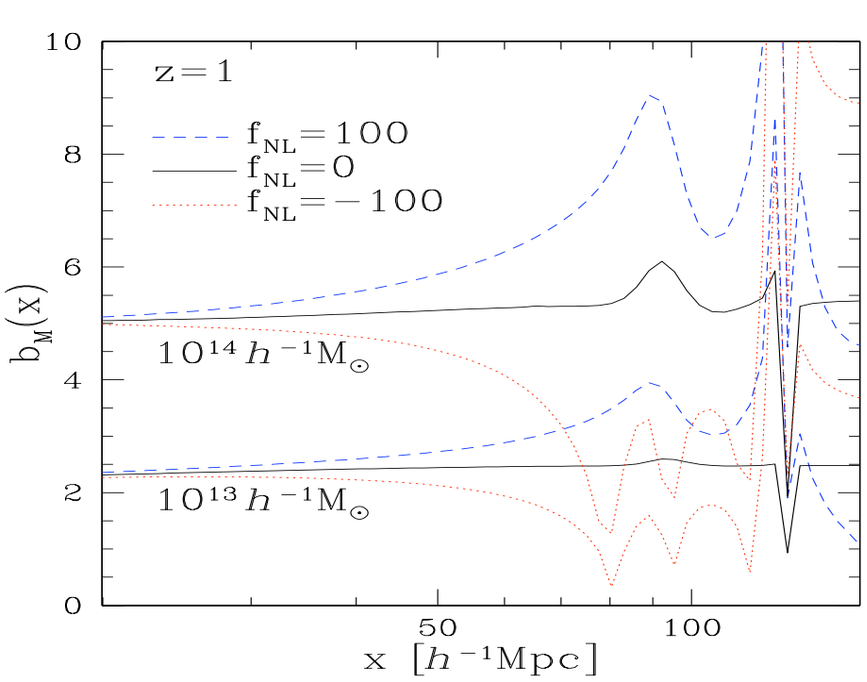

bias $b_M(x)$

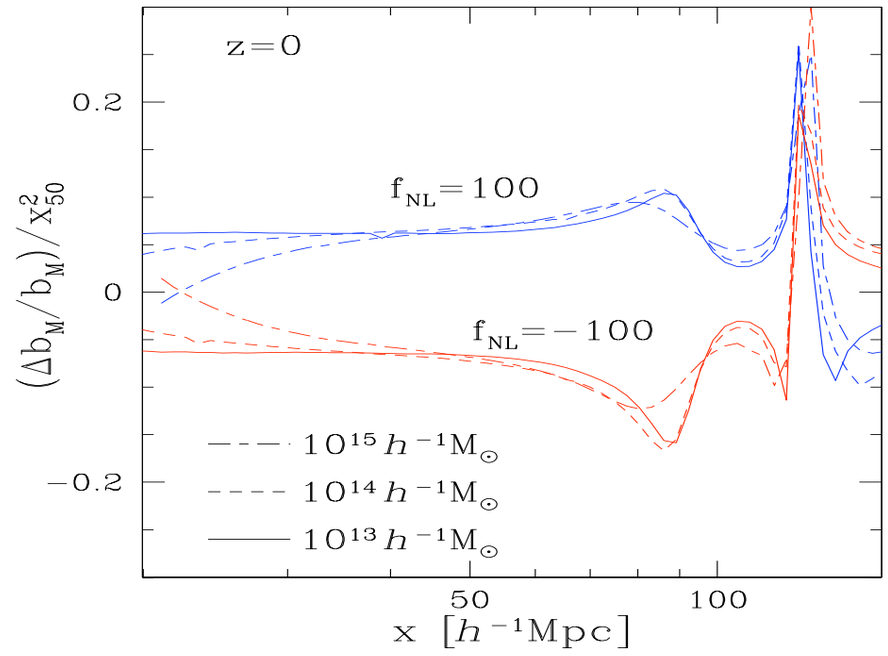

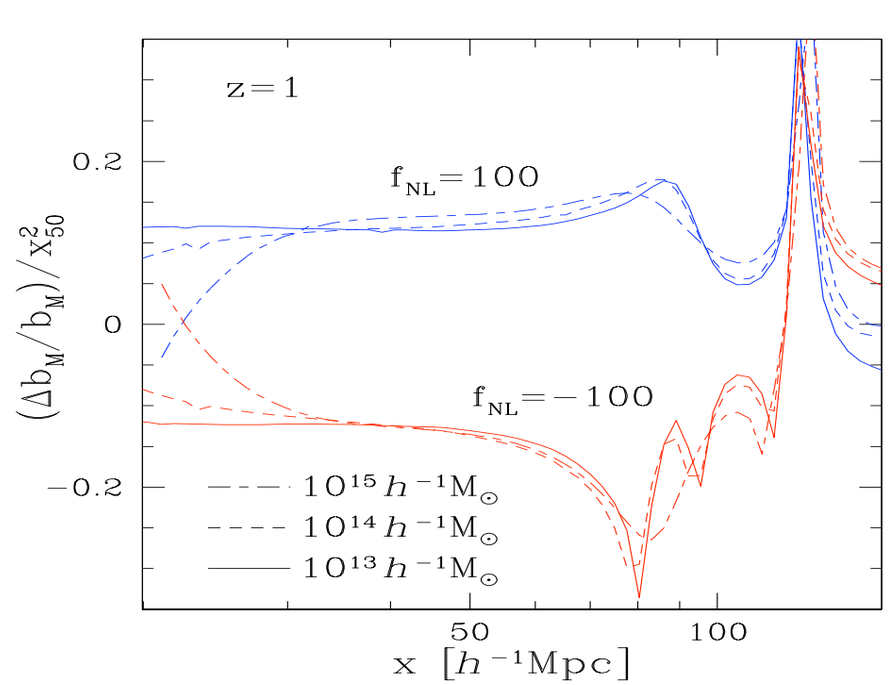

deviation from Gaussian bias,
$\Delta b_M = b_M(f_{\rm NL}) - b_M(f_{\rm NL}=0)$,
scaled by $x^2 b(f_{\rm NL}=0)$

Halo two-point correlation

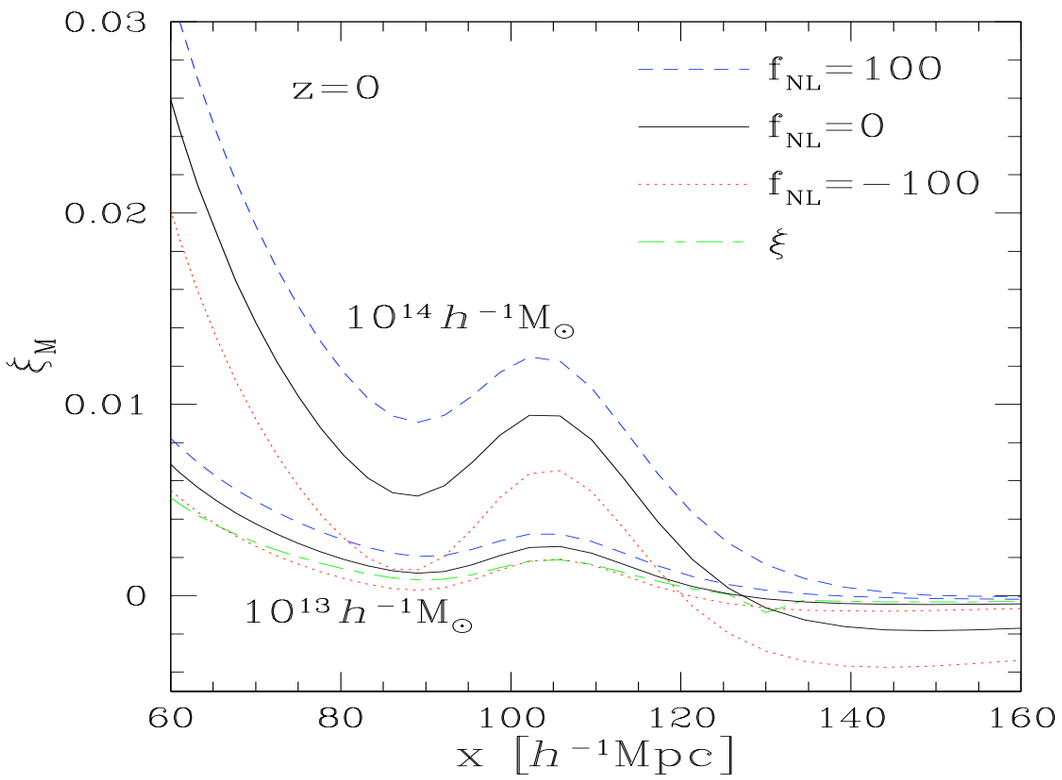

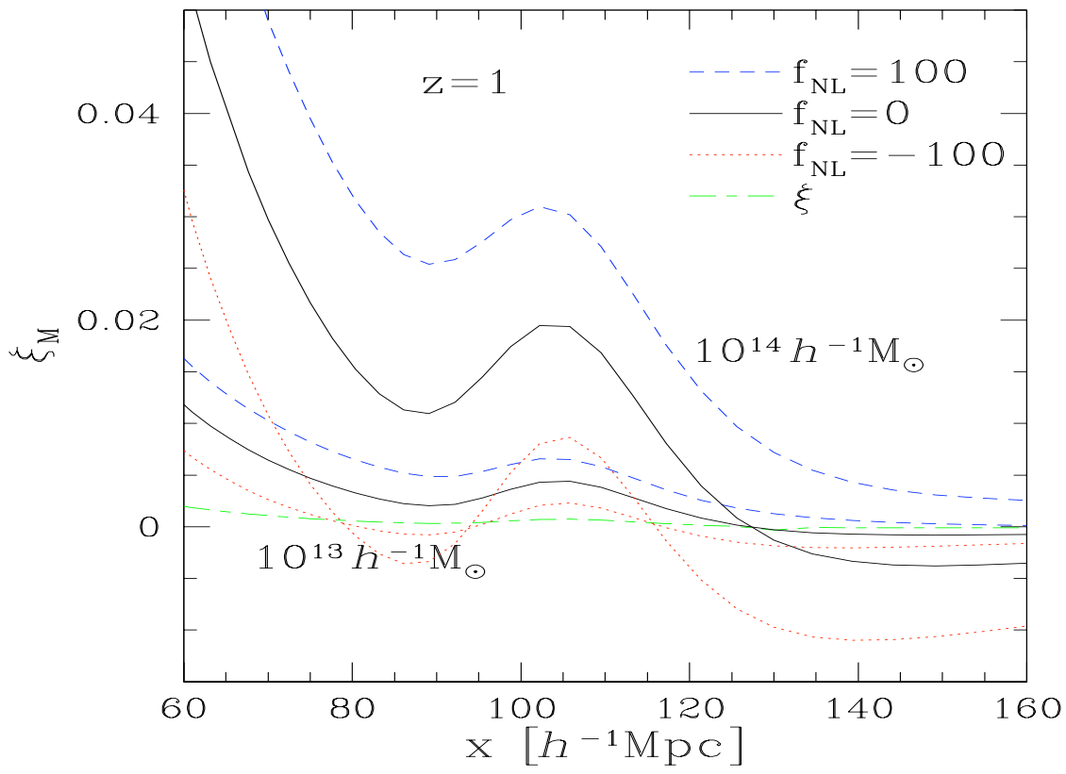

Fourier-space halo power spectrum

Massive halos, low k:

$$b_M(k) \sim \frac{\delta_L}{\sigma_q^2} - 3\frac{\delta_L^2}{\sigma_q^6} f_{1;11} + f_{\rm NL}\frac{2\delta_L^2}{\sigma_q^2 \alpha(k)}$$

constant offset

Slosar et al. (2008)
Desjacques et al. (2009)

k^{-2} large-scale behavior

Dalal et al. (2008)

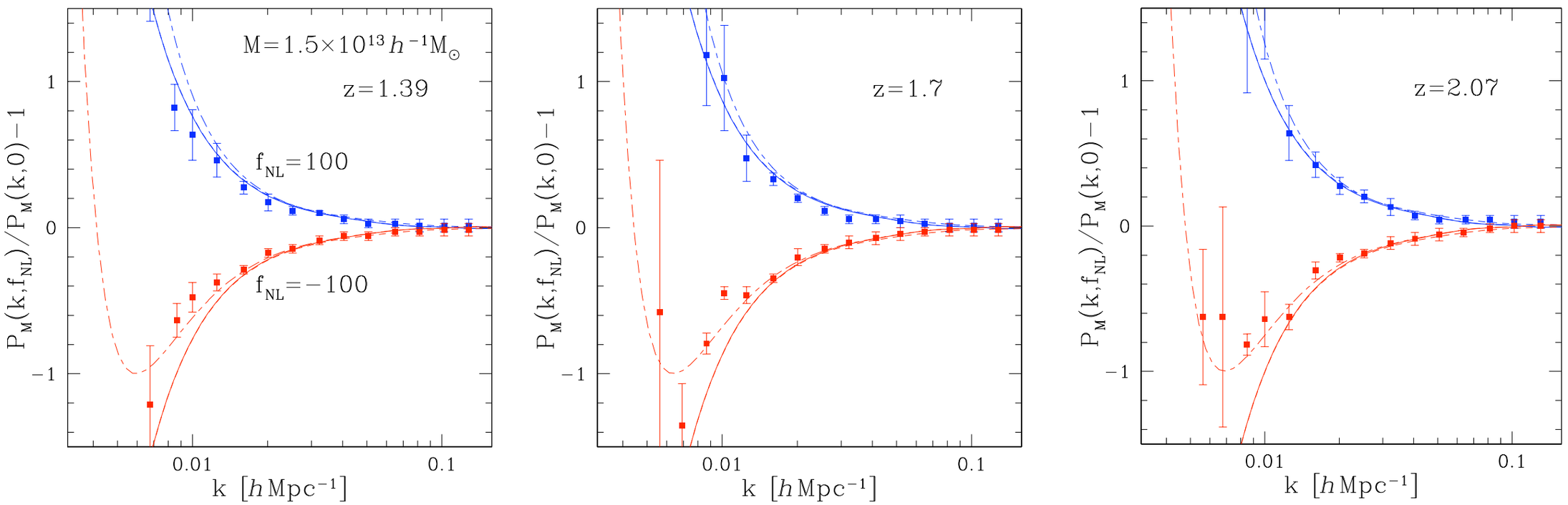

Ratio of non-Gaussian to Gaussian halo power spectra

Desjacques et al. (2009)

Desjacques et al. (2009)

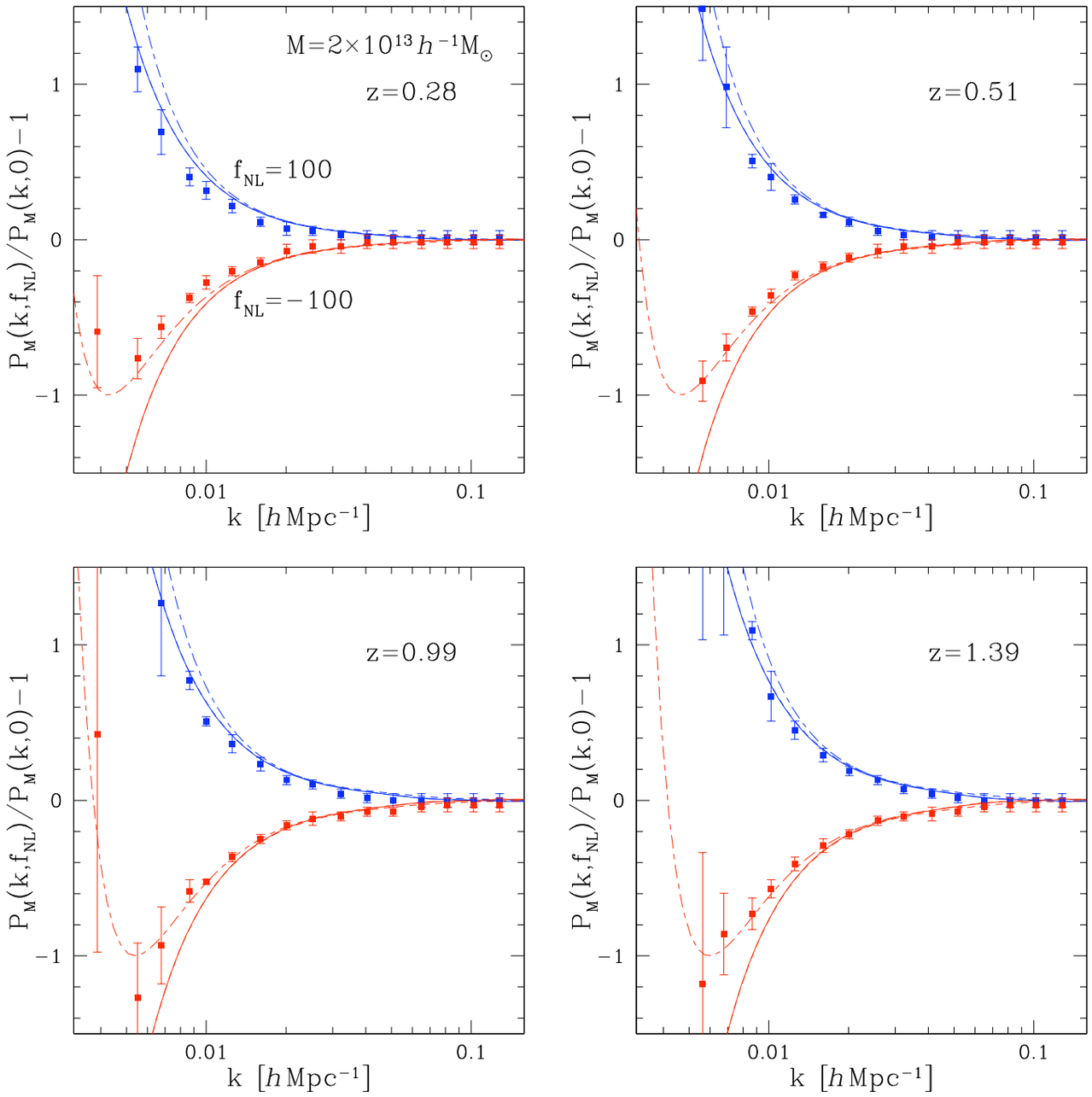

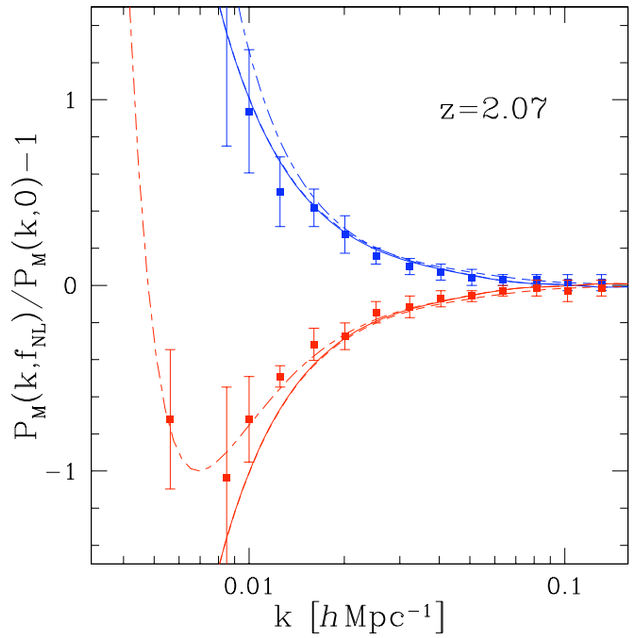

Conclusion

- Upper bound associated with shell-crossing

- Large-mass exponential cutoff of the mass function

- Bias of halos without free parameter, taking into account halo displacement

- This method also applies to non-Gaussian initial conditions

$$\Phi = \phi + \sum_{i=2}^{k} f_i \left(\phi^i - \langle \phi^i \rangle \right)$$

- Large-mass tail of the mass function

- Halo correlation and power spectrum, without free parameters

$$\Delta b(x) \sim x^2 b$$

$$\Delta b(k) \sim f_{\rm NL} \left(1 + \frac{1}{k^2} \right) b(k)$$